ALICE/ITS Note
INT-2000-18
July 11, 2000

Cooling tests for the Silicon Pixel Detectors

F.Scarlassara[1)], A.Pepato[1)], S.Martini[1)], M.Giarin[1)], F.Antinori[1)], N.Carrer[1)], M.Morando[1)], F.Soramel[2)], G.F.Segato[1)], R.Turrisi[1)]

1) Università di Padova, Dip. Fisica "G.Galilei", and INFN Sezione di Padova, Padova, Italy

2) Università di Udine, Udine, Italy and INFN Sezione di Trieste

(July 11, 2000)

Cooling tests have been performed on dummy prototypes of the Silicon Pixel Detector ladders of the Inner Tracking System of Alice, in order to assess the merits of the proposed cooling schemes. The tests provide insight into the problems of cooling of the pixel detectors and also yield experimental parameters necessary for a numerical simulation.

I. INTRODUCTION

The Inner Tracking System (ITS) of the Alice detector is characterized by a relatively large, concentrated power dissipation: a total of 5 kW to 5.5 kW of which 1.5-2 kW are dissipated in the Silicon Pixel Detectors (SPD) alone, which are concentrated in the two innermost barrels [2], corresponding to a power density between 0.55 W/cm^2 and 0.75 W/cm^2. The cooling system has to achieve the required efficiency within the allowed material budget (0.6% X_o) as well as stability and reliability on the long term.

The aim of the cooling tests reported here has been to evaluate the achievable goals within the given boundary conditions, and optimizing heat exchange between the coolant and the detector ladders in the working conditions. However, the above figures for power dissipation are not final yet and differ significantly from the initial estimates of the Technical Proposal (TP) [1], and are dependent on the ongoing development of the pixel chips. The first tests were carried out in agreement with the TP whose specifications foresaw power dissipation of about 8W/stave (see following discussion), while accessibility was to be from one side only. The stated goal was to contain the temperature increase to within 5 ^{o}C. The limited cooling required in that configuration led to the use of a leakless water circuit, operated at pressures P$<$ 1bar. Later on, modifications of the pixel chips raised the power dissipation to somewhere between 25 and 33W/stave [2], thus bringing about a major change in the cooling scheme. One-side access was no longer an option, and the leakless circuit had to be abandoned as well, leading to the alternative choice of fluorocarbon as the coolant fluid. The present note reports on tests performed with both configurations and its structure reflects the history of the tests. Section II gives a short description of the present design of the cooling system, while section III describes the tests with the first setup, using water as a coolant. The tests with the new setup are described in section IV, not only with fluorocarbon coolant (IVb) but also with water (IVa). Discussion of the results follows in section V, together with a summary on the present status and perspectives for the near future.

II. THE COOLING SYSTEM

The SPDs form the 2 inner layers of the ITS, in the shape of two barrels of about 4 cm and 7 cm radius as shown in fig. 1. A barrel is divided into staves (20 staves on the inner barrel and 40 on the external one) which in turn are formed by 4 detector ladders for a total length of 328 mm. They are to be mounted on carbon

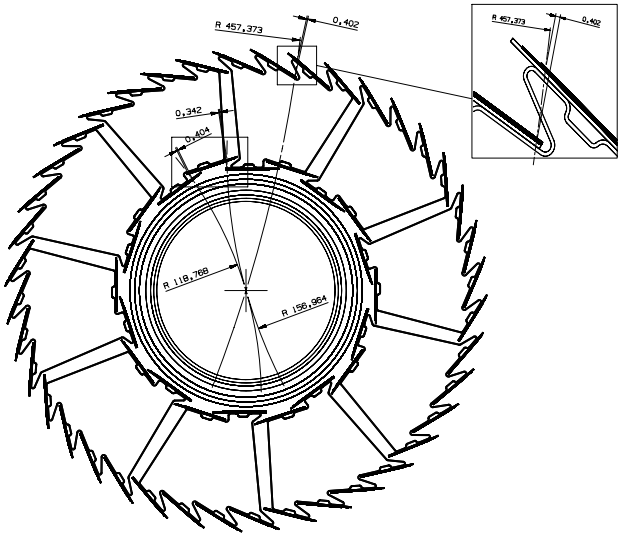

FIG. 1. *Cross section of the SPD barrels. The detectors are distributed in 2 layers of 20 and 40 staves respectively, mounted on 10 carbon-fibre support sectors. Details of the detector mounting with the groove for coolant circulation are also shown.*

support sectors. Two different schemes are being considered for mounting of the detectors and bus: according to the first option the stave bus is directly glued on the carbon sector, followed by the pixel chips and the detector ladders; alternativley, the chips are glued to the carbon fibre, followed by the detector ladders and the bus. The former scenario makes wiring and mounting easier at the expense of a poor thermal coupling between the pixel chips and the cooling channels which are separated by the stave bus. The latter choice favours thermal coupling over mechanical and electrical considerations. Also shown in figure 1 is a magnification of the groove in the carbon support structure for the cooling ducts. Such ducts will be obtained from cylindrical stainless steel tubes with an outer diameter of 2.0 mm to 2.5 mm and a wall thickness of 35 μm squeezed to an internal aperture of 0.6 to 0.8 mm. In the tests, the external diameters before squeezing ranged from 1.5 mm to 3 mm and wall thicknesses of 100 μm. Henceforth, we will refer to the cooling pipes simply by their external diameter before flattening.

III. COOLING TESTS

A. Cooling tests with a one-sided sector

The first setup reflected the conditions specified in the TP, namely low power dissipation (8W/stave) and one-side access to the cooling sectors. Water was chosen as coolant for its efficiency and the cooling circuit operated in the leakless mode. Such a mode of operation greatly reduces the maximum flow that can be achieved but ensures that no liquid leaks onto the sensitive electronics.

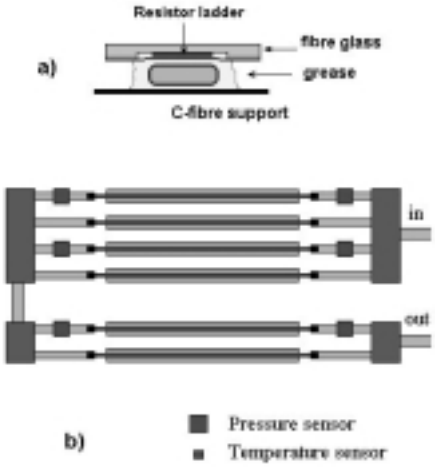

FIG. 2. *a) Cross section of the stave prototype and cooling duct. b) A schematic representation of the 6 dissipators/cooling ducts together with pressure and temperature sensors.*

The cooling efficiency was further reduced by the one-sided approach since the same fluid is used to cool the outer and inner ladders in series. A prototype carbon-fibre sector was employed with the cooling water fed into the 4 ducts on the outer barrel and returning through the 2 ducts on the inner barrel. Since all pipes had the same size, the flow in the inner ducts was double that of the outer ducts. Only the smaller, 1.5 mm ducts were used in the tests. The cooling pipes were laid on the flat surface of the carbon-fibre structure (the prototype sector had no grooves) while the "staves" were kept in position by 1 mm thick spacers. The scheme is illustrated in fig. 2b: a collector on the input side distributed the cooling fluid to the cooling ducts of the 4 outer staves and collected it from the 2 staves of the inner layer. The collector on the other side received the fluid of the outer staves and redistributed it to the inner staves, without external connections. The heating elements were fabricated to simulate each ladder, and having roughly the same size as the stave, which produced a reasonably homogeneous power dissipation.

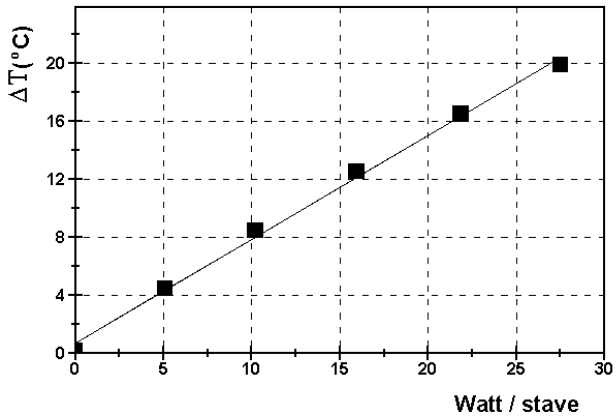

FIG. 3. *Temperature increase as a function of the power per stave for the cooling scheme represented in figure 2. See text for explanations.*

The resistor ladder was on a fibre glass frame as represented in fig. 2a. Thermal coupling between the resistor ladder and the cooling ducts was achieved by means of a conductive grease [1]. During the tests, the whole structure was kept inside a plexiglas cylinder externally lined with an aluminum foil. The temperature was monitored on both sides of each cooling tube by means of 12 Pt100 thermoresistors [2] whereas 6 pressure transducers [3] were positioned at the entrance and exit of 3 tubes. The reduced size of the Pt100 (4x2x0.6 mm^3) and the good thermal contact with the metal surface of the cooling ducts (tightly wound in place by means of thermosetting sleeve) guarantee a reliable temperature reading. Two

[1] Dow Corning 340: thermal conductivity $K \simeq 0.39 W/m^oC$
[2] Tersid mod. MFK 422A TDI
[3] Honeywell Microswitch, 26PCC Type differential gauge.

more Pt100 measured air temperature inside the container. The total temperature increase (ΔT) from input to output is represented in fig. 3 as a function of the power per stave. ΔT increases with power according to the coefficient 0.71 ^{o}C/W. The temperature increase is distributed unequally between the outer and the inner staves: two thirds of it take place in the outer (input) four staves (0.55 ^{o}C/W) and one third in the inner (output) two staves (0.28 ^{o}C/W) due to the double water flux in the latter.
A power dissipation of 8W/stave implies a $\Delta T = 5.7^o$C in cooling water temperature, a value that could have been improved, for instance by use of larger cooling ducts, but the tests were discontinued when the new power figures emerged.

B. Tests with the one-directional setup

1. Water cooling tests.

The efficiency of the setup described in the previous section is inadequate for the presently expected values of power dissipation (25-30 W/stave according to the Technical Design Report [2]). The one-sided approach had to be abandoned in favour of one-way flow (fig. 4).

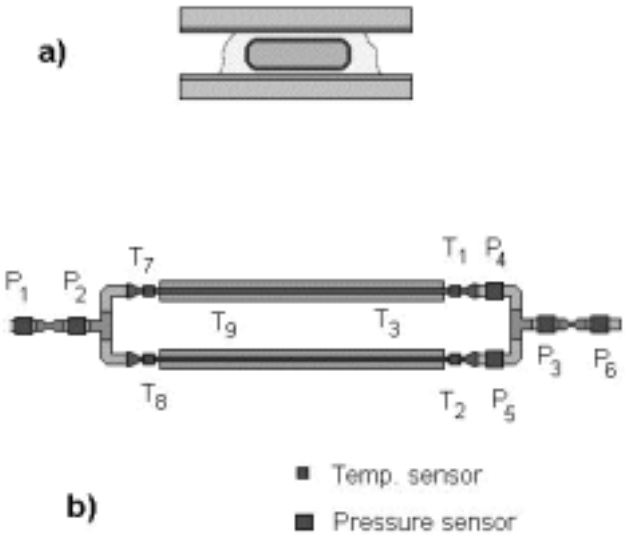

FIG. 4. *Schematic representation of the 2 staves/cooling ducts together with the 3 pressure and 4 temperature sensors. Two more sensors monitored the air temperature inside the container. In the discussion, the coolant is supposed to enter from the left.*

This choice in turn makes the leakless solution impractical since the return hose would have to be about 25 m long and thus limits the flow and cooling efficiency. Therefore an inert fluorcarbon coolant (C_6F_{14}) was chosen instead to limit damage to the electronics in case of leak. Nevertheless, the first tests with the new setup were performed with water, in leakless mode (with a short return hose of about 1 m), in order to compare the two coolants. In the new scheme, an entrance collector distributes the coolant among the 6 tubes of one sector, which take it to an exit collector on the other side of the cooling sector (see [2]). Since all cooling ducts work in parallel, there was no need to use a full prototype sector in that phase of the tests. As can be seen in figure 4, the actual setup was simpler and included only 2 staves with their cooling pipe. The entrance and exit collectors were substituted by simple "tees". Four such prototypes were built in order to test cooling tubes of different sizes (initial diameters 1.5 mm, 2.0 mm, 2.5 mm and 3.0 mm). New distributed resistors, consisting of copper circuits printed on fibre glass frames, were employed in the tests. Because of power limitations a cooling duct was sandwitched between two such resistors. The thermal coupling is thus enhanced compared to working conditions due to:
a) doubling the contact surface, now on both sides of the cooling pipe and
b) insulating the power source towards the exterior by means of the thick (1 mm) fibre glass support.
The two staves lay on a carbon fibre support, and the full setup was enclosed in a 3 cm thick insulating polyurethane box, internally lined with a thin Al sheet. The only apertures were those strictly required for coolant flow and electric wiring (for the resistors and the sensing devices) thus providing an effective thermal insulation (the thermal resistance in the absence of flow was about 30 ^{o}C/W). In view of point a) tests with such a prototype should provide an optimistic result as regargds the maximal ΔT along a stave. On the other hand one can reliably equate the dissipated power of the resistor and the power removed by the coolant, in steady state conditions.

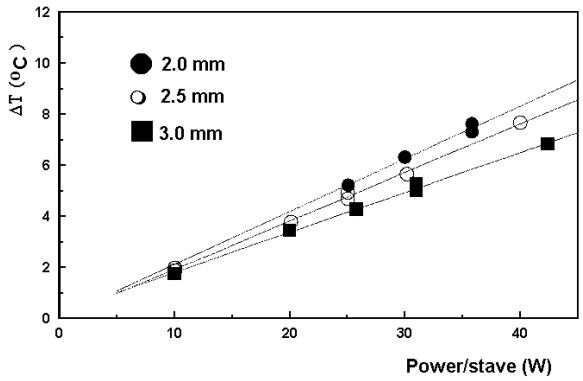

FIG. 5. ΔT *as a function of the power dissipated per stave using the setup of fig. 4 with water cooling. The lines are linear fits to the data.*

The arrangement of Pt100 is similar to the one of the Pt100 temperature sensors described in the previous

paragraph, whereas the arrangement of pressure sensors is more complex (fig. 4b). Both sensors were of the same type as in section III.A. If the pressure drop along the flat portion of the ducts (in thermal contact with the dissipator) is needed, corrections must be applied to the measured difference $P_2 - P_3$, to properly correct for the effect of the changes in cross section of the cooling duct (circular to flat, and viceversa) and the two "tees". The first effect was measured at the sides of a short portion (1 cm) of pipe undergoing such changes while the pressure drop at the "tee" (e.g. $(P_4 + P_5)/2 - P_3$) was approximately 50% larger than the former.
The results of the water tests for different diameters of the cooling ducts are summarized in fig. 5. The improvement, if compared with fig. 3 is apparent. ΔT is now well below 10 ^{o}C for a 1.5 mm pipe, even at the upper limit of 33 W/stave. Even better performances are achieved with larger tubes.

2. fluorocarbon cooling tests

The same apparatus has been tested at CERN with fluorocarbon [4] as coolant. Such tests were performed at $P > 1$ bar, as previously explained. That choice was also forced by the lower specific heat and larger viscosity of the fluorocarbon compared to water. Because of the new degree of freedom (flow could not be varied in practice during the water-cooling tests) the fluorocarbon-cooling tests have been more extensive and cover different flows for a given set of cooling ducts.

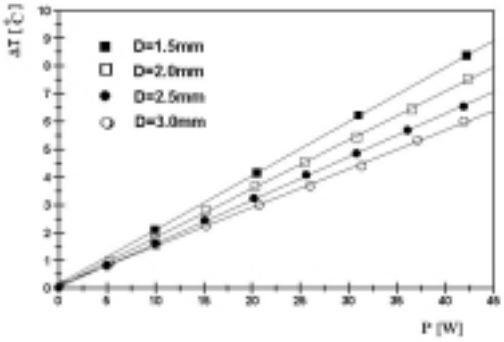

FIG. 6. *ΔT vs power per stave with C_6F_{14} coolant. The configuration is the one represented in figure 4.*

The most detailed tests were performed with the 2.5 mm and 3.0 mm pipes. Fig. 6 summarizes the results obtained with the different tubes when the total pressure drop $(P_2 - P_3)$ was about 1 bar, whereas in fig. 7a one finds a summary of the cooling tests performed with the 3.0 mm ducts at three different flows. The reason for fixing the pressure difference at this level was twofold: for lower flows the two cooling ducts may not behave in the same way, (e.g. $\Delta T_1 = T_1 - T_7$ may differ from $\Delta T_2 = T_2 - T_8$ by more than 1 ^{o}C at the lower flows); on the other hand larger pressures might have deformed the flat ducts, and our sensors were limited to ± 1 bar.

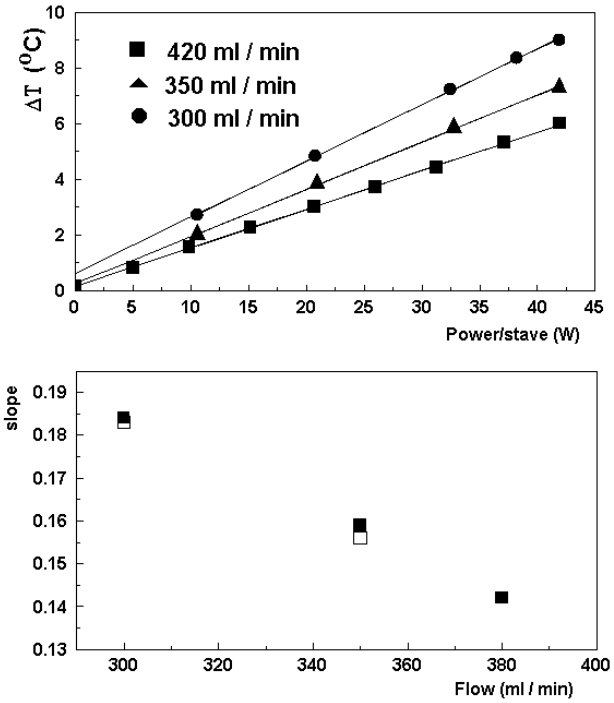

FIG. 7. *Effects of flow on the cooling efficiency of the setup in fig. 4 with 3.0 mm tubes. Top panel: ΔT vs Power/stave. Bottom panel: slope vs flow.*

In figs.6 and 7 $\Delta T = (\Delta T_1 + \Delta T_2)/2$ is plotted versus power/stave. Comparison of fig. 6 with fig. 5 reveals a slight improvement relative to water, in particular for the smaller ducts. The inlet fluorocarbon temperature was also varied in the tests (10^{o}C and 20^{o}C), but as expected, ΔT does not depend on the inlet temperature, as one can appreciate in fig. 7b reporting the slope of the plot ΔT vs power/stave (in ^{o}C/W) as measured with different flows and different input temperatures: the full squares correspond to inlet temperatures of 20^{o}C and the blank squares to inlet temperatures of 10^{o}C. All points in fig. 6 and fig. 7a correspond to an inlet temperature of 20^{o}C.

IV. DISCUSSION AND CONCLUSIONS

The results reported above are only concerned with the temperature increase of the coolant between entry and exit of the pixel stave but that is not the only interesting

[4] C_6F_{14}, 3M^{TM}'s perfluorocarbon PF-5060

aspect regarding temperature increase. It goes without saying that the ladder itself must be hotter than the cooling fluid and, in an thermally insulated environment, one can expect the air to stabilize at an intermediate temperature between coolant and ladder.

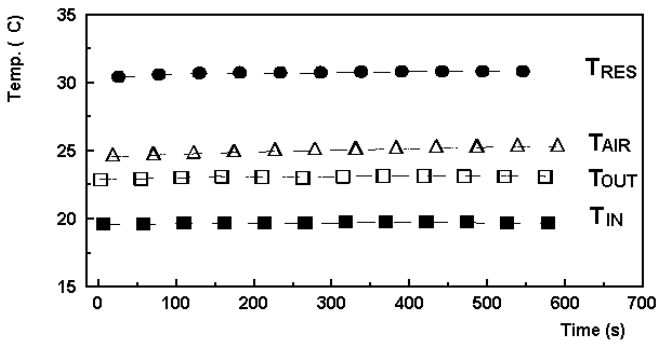

FIG. 8. *Time dependence of the water temperature (entrance and exit), air temperature and ladder temperature. Notice that the air in the insulated box heats more than the cooling fluid.*

This is indeed what is observed, as can be judged in fig. 8 reporting the time dependence of input and output temperatures of the cooling water, the air temperature (average of two measurements, from Pt100's placed about 5 cm above the ladders, close to its extremities) and the "ladder temperature". The ladder temperature is the average of 4 temperature measurements along the resistor

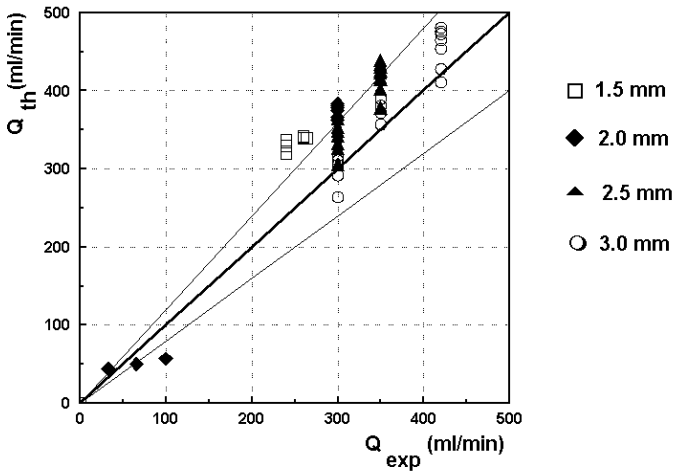

FIG. 9. *Calculated flow (Q_{th}) vs measured flow (Q_{exp}) in the fluorocarbon tests. Q_{th} is calculated from thermal balance. The lines represent $Q_{th} = Q_{exp}$ together with $\pm 20\%$ deviations.*

(Cu printed circuit boards). The Pt100's for this measurement were placed at almost regular intervals along the ladder, and were consistent with a constant temperature. Fluctuations being mainly due to the difficulty of getting good thermal contact with the Cu-resistors while avoiding the ubiquitous conductive grease in contact with the cooling ducts. Since the system is insulated the power dissipated in the resistors equals the power removed by the fluid ($W_F = \delta \cdot Q \cdot \Delta T$, δ being the fluid density and Q the flow).

Fig. 9 shows that this is indeed the case in the fluorocarbon tests since most points fall within 20% from the flowmeter [5] reading. In the water tests, the flow was not measured directly, but was estimated from thermal balance. The values thus obtained range from 40 to 80 ml/min, with Reynolds numbers $550 < Re < 750$, indicative of laminar flow.

The fluorocarbon flow, on the other hand, is characterized by $3000 < Re < 5000$, too large for a laminar flow ($Re < 1000$), but not yet in the turbulent regime ($Re > 10000$). With this coolant, a few points were actually measured at lower flow: they are reported in figs. 9 and 10, but not in figs. 6 and 7. As a way to visualize the flow regime one can compare the data with laminar-flow (Poiseuille like) calculations. Our squeezed ducts have a non standard shape, however it is reasonable to approximate the flow in the rectangular portion of the cross section as if it were a portion of flow between two infinite parallel surfaces. In such an approximation, the flow can be expressed as:

$$Q = \frac{ah^3}{12\eta}\frac{\Delta P}{\ell}$$

where a is the width of the rectangular portion, h the distance between the parallel planes and η is the dynamical viscosity. ΔP is the pressure drop across the cooling ducts as discussed above. The comparison in figure 10 is between experimental pressure drops (ΔP_{exp}) and that calculated with the above formula for a laminar regime (ΔP_{th}).

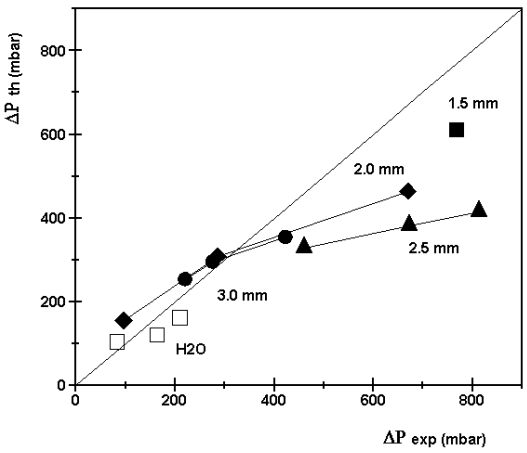

FIG. 10. *Calculated versus measured flow. C_6F_{14} data.*

[5] Flowmeter model SFL from Kobold instruments

The prototypes utilized so far are still some way from a realistic test in working conditions. They have helped to decide on which type of cooling system should be implemented in the Alice ITS pixel detectors, and provide crucial data for future simulations. They also raise some question on the very definition of acceptable temperature increase within the SPD barrels: is it sensitive to refer to the heating of the coolant, or should one rather talk about ambient (i.e. air) heating? After all it is the latter that matters to the neighbouring ITS detectors (the Silicon Drift Detectors, SDD), but the former is easier to measure and control. Since one cannot prevent a fraction of the power dissipated from propagating radially to the external ITS layers, the cooling scheme of the SPD will be completed by an external carbon-fibre shield which may carry additional air cooling and/or liquid cooling ducts. Such an arrangement should provide better temperature uniformity towards the SDD layers. New tests are in preparation with a more realistic setup, using a couple of carbon-fibre sectors complete with their 10 "barrels" with cooling ducts and the external shield. Besides being more realistic, such tests will provide information on the temperature uniformity achievable on the external shield, a crucial parameter for the neighbouring detectors of the ITS. Another important issue to address is concerned with the final choice of the ladder-bus mounting (the two options mentioned in sec. II). The feasibility of the first option, on thermal grounds, depends crucially on the results of the forthcoming tests.

V. ACKNOWLEDGMENTS

We gratefully acknowledge the help and support of M.Bosteels who helped us set up the apparatus at LNL, and again M.Bosteels and A.Onnela who also allowed us to use their pumping system at CERN with the fluorocarbon coolant and were very supportive during the preparation of those tests.

---

[1] ALICE
Technical Proposal, CERN/LHCC 95-71, LHCC/P3 15-12-1995

[2] Alice Inner Tracking System, Technical Design Report, CERN/LHCC 99-12 ALICE TDR 4, 18 June 1999